Journal of King Saud University – Engineering Sciences (2016) **xxx**, xxx–xxx

King Saud University

Journal of King Saud University – Engineering Sciences

www.ksu.edu.sa
www.sciencedirect.com

ORIGINAL ARTICLES

The influence of membrane excitations on bioethanol production in a forced fermentor

M.E.E. Abashar

Department of Chemical Engineering, College of Engineering, King Saud University, P.O. Box 800, Riyadh 11421, Saudi Arabia

Received 10 June 2016; accepted 17 October 2016

KEYWORDS

Bioethanol;
Chaos;
Hyperchaos;
Membrane excitations;
Quasi-periodicity

Abstract Modeling and numerical simulation are implemented to investigate the influence of membrane excitations on the production of bioethanol in a forced fermentor. Three well developed attractors in the frequency locking, quasi-periodic and chaotic regions are subjected to membrane excitations. Two membrane configurations are employed for each case: the shock type and the linear dynamic membranes. It is interesting that all membrane configurations exhibit wealthy regions of complex dynamics and very beneficial to the fermentor performance. The simulated results reveal various fascinating phenomena such as hyperchaos, chaos and large bubble windows. It was shown that the chaotic regions are the attractive and best potential regions for the implementation of the membrane excitations. It is interesting to note that when the shock type and linear membranes are imposed on chaotic regions, the hyperchaotic attractors arise and have substantial impact in increasing the average ethanol yield to 18.98% and 19.29%, respectively. It is obvious that the linear dynamic membranes are superior to the shock type membranes with respect to the bioreactor performance. The bubble windows show an incomplete odd sequence of bubble birth of 1, 3 and 5 bubbles.

© 2016 The Author. Production and hosting by Elsevier B.V. on behalf of King Saud University. This is an open access article under the CC BY-NC-ND license (http://creativecommons.org/licenses/by-nc-nd/4.0/).

1. Introduction

There has been growing interest to understand the dynamic behavior and the associated nonlinear phenomena of biological reactors (Abashar and Elnashaie, 2011; Abashar, 2012, 2011; Bruce et al., 1991; Cristina et al., 2011; Garhyan and Elnashaie, 2004a,b; Jobses et al., 1986, 1985; Parulekar, 2001, 1998; Sinčić and Bailey, 1980; Villadsen et al., 2011). It is well known that the efficient design, operation, control and performance of chemical reactors are profoundly affected by the dynamic phenomena and the related parameter space (Abashar, 1994; Kevrekidis and Aris, 1986; Kevrekidis et al., 1986; Mankin and Hudson, 1984). The nonlinear phenomena can be attractive and beneficial to enhance the yield and selectivity of products or can be harmful and in this case proper control actions are needed to be taken (Abashar and Elnashaie, 2010; Abashar, 1994). The compelling interest of the bioreactor designers in the nonlinear phenomena necessitates extensive parameter space exploration coupled with a deeper fundamental understanding. Bifurcation, catastrophe, singularity and chaos theories have played a central role in this

Peer review under responsibility of King Saud University.

ELSEVIER Production and hosting by Elsevier

http://dx.doi.org/10.1016/j.jksues.2016.10.004
1018-3639 © 2016 The Author. Production and hosting by Elsevier B.V. on behalf of King Saud University.
This is an open access article under the CC BY-NC-ND license (http://creativecommons.org/licenses/by-nc-nd/4.0/).

Nomenclature

Notation

a'	constants in Eq. (14a), m^2
a''	constant in Eq. (14b), m^2/h
a	constants in Eq. (21b), m^2
A'	forcing amplitude, kg/m^3
A_p	permeation area, m^2
C_i	concentration of component i, kg/m^3
C_{sf}	periodic substrate feed concentration, kg/m^3
C_{so}	substrate feed concentration, kg/m^3
D	dilution rate, h^{-1}
k	membrane permeability, m/h
k_1	empirical constant, h^{-1}
k_2	empirical constant, $m^3/kg\ h$
k_3	empirical constant, $m^6/kg^2\ h$
K_s	Monod constant, kg/m^3
m_s	maintenance factor based on substrate requirement, kg/kg h
m_p	maintenance factor based on product formation, kg/kg h
P	rate constant, h^{-1}
q	volumetric flowrate, m^3/h
t	time, h
V	volume, m^3
Y_p	ethanol yield, kg/kg
$\bar{Y}_P$	average ethanol yield, kg/kg
Y_{sx}	yield factor of biomass on substrate, kg/kg
Y_{px}	yield factor of biomass on product, kg/kg
Z	dimensionless concentration

Greek letters

λ_i	ith Lyapunov exponent
ρ	ethanol density, kg/m^3
τ	dimensionless time
$\acute{\omega}$	forcing frequency, rad/h

respect (Jackson, 1989; Kevrekidis and Aris, 1986; Kevrekidis et al., 2007, 1986; Taylor et al., 1993).

Several investigations have shown that the bioethanol reactor exhibits complex dynamic behavior with a wide variety of fascinating nonlinear dynamic phenomena such as multiplicity of steady states, quasi-periodicity, chaos and multi-stability (Abashar, 2012, 2011; Garhyan and Elnashaie, 2004a,b). However, the bioethanol reactor suffers from a serious problem of the ethanol inhibition of fermentation microorganisms. Many researchers have reported that the in situ removal of the ethanol using a permselective membrane has a significant effect to minimize ethanol inhibition and to enhance the ethanol yield (Garhyan and Elnashaie, 2004a,b; Ikegami et al., 1997; Nomura et al., 2002). The membranes also have been utilized to separate and recycle microorganism cells to the bioreactor in order to enhance the bioethanol production (Nishiwaki and Dunn, 1999).

The membrane excitations means, the disturbance of the membrane by altering its state dynamically are extremely scarce subject in the literature. The purpose of this work is to explore and reveal for the first time the dynamic sequence of events happen and the possible dynamic phenomena might arise when the sinusoidally forced bioethanol fermentor is subjected to membrane excitations. Evaluation of the potential benefits of the membrane excitations from fundamental and practical standpoints is also explored.

2. Bioreaction kinetics

Jobses et al. (1985, 1986) reported the bioreaction kinetics for bioethanol formation by *Z. mobilis* as follows:

$$r_x = \mu C_x \tag{1}$$

$$r_s = \frac{r_x}{Y_{sx}} + m_s C_x = \left[\frac{\mu}{Y_{sx}} + m_s\right] C_x \tag{2}$$

$$r_p = \frac{r_x}{Y_{px}} + m_p C_x = \left[\frac{\mu}{Y_{px}} + m_p\right] C_x \tag{3}$$

$$r_e = \left[\frac{(k_1 - k_2 C_p + k_3 C_p^2)}{K_s + C_s}\right] C_s C_e \tag{4}$$

$$\mu = \frac{\mu_{\max} C_s}{(K_s + C_s)} \tag{5}$$

where r_x, r_s, r_p, r_e are the rates of biomass growth, substrate consumption, ethanol production and key component formation, respectively; C_x, C_s, C_P, C_e are the concentrations of the biomass, substrate, bioethanol and key component, respectively; k_{1-3} are rate constants. Y_{sx}, Y_{px} are the yield factor of biomass on the substrate and product, respectively; m_s, m_p are the maintenance factor for substrate and product formation, respectively; $\mu_{\max}$ is the maximum specific growth rate and K_s is the Monod constant.

The bioethanol inhibition mechanism is offered by Jobses et al. (1985, 1986) as follows: the formation of an internal key component (e) such as RNA (ribonucleic acid) or protein produces the maximum growth rate of the biomass. The formation of the bioethanol inhibits the formation of the internal key component and the growth rate of the biomass to attain the maximum rate.

3. Formulation of reactor model

A schematic diagram of the bioreactor-separator system with a membrane is depicted in Fig. 1. The dynamics of this system is described by a set of ordinary differential equations as follows (Abashar, 2011; Jobses et al., 1986, 1985):

Reactor:

Biomass:

$$\frac{dC_{x_1}}{dt} = \frac{P C_{s_1} C_{x_1}}{(K_s + C_{s_1})} - \frac{q_1}{V_1} C_{x_1} \tag{6}$$

Substrate

$$\frac{dC_{s_1}}{dt} = D_1 C_{sf} - \frac{q_1}{V_1} C_{s_1} - \left[\frac{P}{Y_{sx}} \frac{C_{s_1} C_{e_1}}{(K_s + C_{s_1})} + m_s C_{x_1}\right] \tag{7}$$

Please cite this article in press as: Abashar, M.E.E. The influence of membrane excitations on bioethanol production in a forced fermentor. Journal of King Saud University – Engineering Sciences (2016), http://dx.doi.org/10.1016/j.jksues.2016.10.004

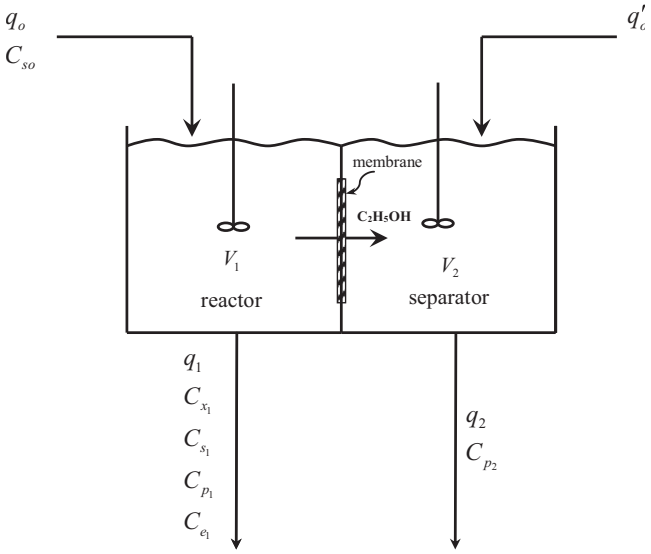

Figure 1 Schematic diagram of a membrane bioreactor-separator system.

Ethanol

$$\frac{dC_{p_1}}{dt} = \left[\frac{P}{Y_{px}}\frac{C_{s_1}C_{e_1}}{(K_s + C_{s_1})} + m_p C_{x_1}\right] - \frac{q_1}{V_1}C_{p_1} - \frac{k\,A_p}{V_1}(C_{p_1} - C_{p_2}) \tag{8}$$

Key component

$$\frac{dC_{e_1}}{dt} = \left[\frac{\left(k_1 - k_2 C_{p_1} + k_3 C_{p_1}^2\right)}{(K_s + C_{s_1})}\right] C_{s_1} C_{e_1} - \frac{q_1}{V_1}C_{e_1} \tag{9}$$

Separator:

$$\frac{dC_{p_2}}{dt} = \frac{k\,A_p}{V_2}(C_{p_1} - C_{p_2}) - \frac{q_2}{V_2}C_{p_2} \tag{10}$$

The kinetic parameters are shown in Table 1. The feed concentration to the bioreactor is introduced sinusoidally as follows:

$$C_{sf} = C_{so} + A' \sin \omega' t \tag{11}$$

where $\acute{A}$ is the forcing amplitude and ώ is the forcing frequency. The exit volumetric flow rates from the bioreactor and the separator are given by:

$$q_1 = q_o - \frac{k\,A_p}{\rho}(C_{p_1} - C_{p_2}) \tag{12}$$

Table 1 Kinetics parameters (Abashar, 2012, 2011; Garhyan and Elnashaie, 2004a,b).

Parameter	Value
k_1 (h^{-1})	16.0
k_2 (m^3/ kg h)	4.97×10^{-1}
k_3 (m^6/ kg^2 h)	3.83×10^{-3}
K_s (kg/ m^3)	0.5
m_s (kg/kg h)	2.16
m_p (kg/kg h)	1.1
P (h^{-1})	1.0
Y_{sx} (kg/kg)	2.44498×10^{-2}
Y_{px} (kg/kg)	5.26315×10^{-2}

$$q_2 = q'_o + \frac{k\,A_p}{\rho}(C_{p_1} - C_{p_2}) \tag{13}$$

where A_p is the membrane permeation area, k is the permeability of the membrane and ρ is the density of ethanol. The bioreactor is excited by the membrane according to the following turn on relations:

$$A_p\,H(t - t_{open}) = \begin{cases} 0, & t < t_{open} \\ A_p = a', & t \geqslant t_{open} \end{cases} \tag{14a}$$

$$A_p(t - t_{open})\,H(t - t_{open}) = \begin{cases} 0, & t < t_{open} \\ A_p = a''(t - t_{open}), & t \geqslant t_{open} \end{cases} \tag{14b}$$

where $H(t)$ denotes the Heaviside function. For convenience, we introduce the flowing dimensionless quantities to normalize the equations:

$$\begin{aligned}
&Z_1 = \frac{C_{x_1}}{C_{ref}}; \quad Z_2 = \frac{C_{s_1}}{C_{ref}}; \quad Z_3 = \frac{C_{p_1}}{C_{ref}}; \quad Z_4 = \frac{C_{e_1}}{C_{ref}}; \\
&Z_5 = \frac{C_{p_2}}{C_{ref}}; \quad Z_{2f} = \frac{C_{s_o}}{C_{ref}}; \quad \alpha_1 = \frac{q_o P_o}{V_1}; \quad \alpha_2 = P P_o; \\
&\alpha_3 = \frac{P P_o}{Y_{sx}}; \quad \alpha_4 = P_o m_s; \quad \alpha_5 = \frac{P P_o}{Y_{px}}; \quad \alpha_6 = P_o m_p; \\
&\gamma_1 = \frac{P_o k C_{ref}}{V_1 \rho}; \quad \gamma_2 = \frac{P_o k}{V_1}; \quad \theta_1 = \frac{V_1}{V_2}; \quad \theta_2 = \frac{q'_o}{q_o}; \\
&\omega = \omega' P_o; \quad \tau = \frac{t}{P_o}; \quad a = a'' P_o; \quad A = \frac{\alpha_2 A'}{C_{ref}}; \\
&k'_1 = k_1 P_o; \quad k'_2 = k_2 P_o C_{ref}; \quad k'_3 = k_3 P_o C_{ref}^2; \\
&K = \frac{K_s}{C_{ref}}
\end{aligned} \tag{15}$$

Hence, the ordinary differential equations for the bioreactor and separator are cast into the following equations:

$$\frac{dZ_1}{d\tau} = -\alpha_1 Z_1 + \frac{\alpha_2 Z_2 Z_4}{[K + Z_2]} + \gamma_1 A_p Z_1 (Z_3 - Z_5) \tag{16}$$

$$\frac{dZ_2}{d\tau} = \alpha_1(Z_{2f} - Z_2) + A \sin \omega\tau - \left[\alpha_3 \frac{Z_2 Z_4}{(K + Z_2)} + \alpha_4 Z_1\right] + \gamma_1 A_p Z_2 (Z_3 - Z_5) \tag{17}$$

$$\frac{dZ_3}{d\tau} = -\alpha_1 Z_3 + \left[\alpha_5 \frac{Z_2 Z_4}{(K + Z_2)} + \alpha_6 Z_1\right] + (\gamma_1 Z_3 - \gamma_2) A_p (Z_3 - Z_5) \tag{18}$$

$$\frac{dZ_4}{d\tau} = -\alpha_1 Z_4 + \left[\frac{(k'_1 - k'_2 Z_3 + k'_3 Z_3^2)}{(K + Z_2)}\right] Z_2 Z_4 + \gamma_1 A_p (Z_3 - Z_5) Z_4 \tag{19}$$

$$\frac{dZ_5}{d\tau} = -\alpha_1 \theta_1 \theta_2 Z_5 + \theta_1 A_p (\gamma_2 - \gamma_1 Z_5)(Z_3 - Z_5) \tag{20}$$

and the membrane functions become:

$$A_p\,H(\tau - \tau_{open}) = \begin{cases} 0, & \tau < \tau_{open} \\ A_p = a', & \tau \geqslant \tau_{open} \end{cases} \tag{21a}$$

$$A_p(\tau - \tau_{open})\,H(\tau - \tau_{open}) = \begin{cases} 0, & \tau < \tau_{open} \\ A_p = a(\tau - \tau_{open}), & \tau \geqslant \tau_{open} \end{cases} \tag{21b}$$

The ethanol yield is given by:

$$Y_P = \frac{(q_1 C_{p1} + q_2 C_{p2})}{q_o C_{so}} = \frac{(\theta_3 Z_3 + \theta_4 Z_5)}{Z_{2f}} \tag{22}$$

and the average ethanol yield is given by:

$$\bar{Y}_p = \frac{\int_{\tau_1}^{\tau_2} Y_p d\tau}{\tau_2 - \tau_1} \tag{23}$$

4. Computational algorithms

The system of the ordinary differential equations are solved by a Fortran subroutine for solving stiff differential equations called Dgear from the IMSL (International Mathematics and Statistics Library) with automatic step size and double precision were used with input relative error bound of 10^{-14}. The Poincaré bifurcation diagram is constructed by employing the forcing period to strobe the system. The eigenvalues are computed by using an IMSL subroutine called Eigrf. The Gram-Schmidt reorthonormalization (GSR) procedure is used to compute the Lyapunov exponents. The figures are prepared by the Golden Software Grapher 5.

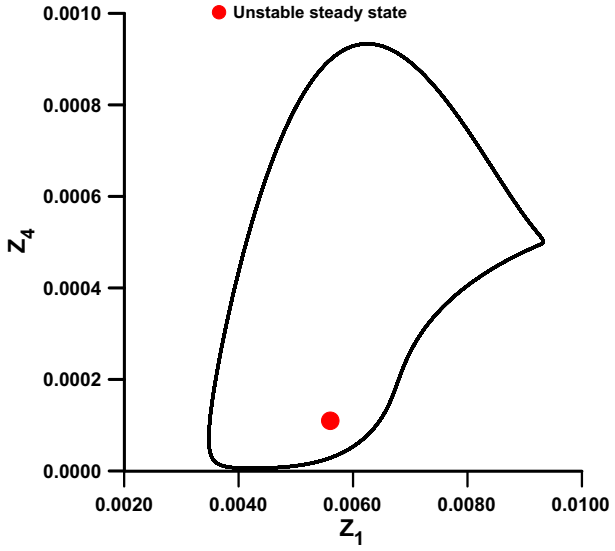

Figure 2 The autonomous (unforced system) limit cycle.

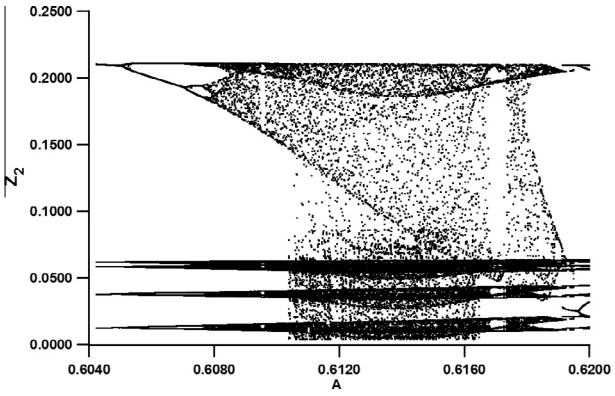

Figure 3 A one-parameter stroboscopic Poincaré bifurcation diagram for the forced system without membrane for $A = 0.6040$–0.6200.

5. Results and discussion

5.1. Steady state autonomous bioethanol fermentor without membrane

For the autonomous reactor at steady state conditions and without membrane the following parameters are set to zero ($A = 0$, $A_p = 0$). The steady state equations of the reactor after lengthy manipulation are reduced to the following cubic polynomial:

$$\phi_3 Z_2^3 + \phi_2 Z_2^2 + \phi_1 Z_2 + \phi_0 = 0 \tag{24}$$

where:

$$\begin{aligned}
\phi_0 &= -\alpha_1 K,\\
\phi_1 &= k_1' - \alpha_1 - k_2' Z_{2f} \frac{\left[\frac{\alpha_5}{\alpha_2} + \frac{\alpha_6}{\alpha_1}\right]}{\left[\frac{\alpha_3}{\alpha_2} + \frac{\alpha_4}{\alpha_1}\right]} + k_3' Z_{2f}^2 \frac{\left[\frac{\alpha_5}{\alpha_2} + \frac{\alpha_6}{\alpha_1}\right]^2}{\left[\frac{\alpha_3}{\alpha_2} + \frac{\alpha_4}{\alpha_1}\right]^2},\\
\phi_2 &= k_2' \frac{\left[\frac{\alpha_5}{\alpha_2} + \frac{\alpha_6}{\alpha_1}\right]}{\left[\frac{\alpha_3}{\alpha_2} + \frac{\alpha_4}{\alpha_1}\right]} - 2k_3' Z_{2f} \frac{\left[\frac{\alpha_5}{\alpha_2} + \frac{\alpha_6}{\alpha_1}\right]^2}{\left[\frac{\alpha_3}{\alpha_2} + \frac{\alpha_4}{\alpha_1}\right]^2},\\
\phi_3 &= k_3' \frac{\left[\frac{\alpha_5}{\alpha_2} + \frac{\alpha_6}{\alpha_1}\right]^2}{\left[\frac{\alpha_3}{\alpha_2} + \frac{\alpha_4}{\alpha_1}\right]^2}
\end{aligned} \tag{25}$$

The roots of Eq. (24) are obtained by following equations:

$$\begin{aligned}
Z_{21} = &-\frac{\phi_2}{3\phi_3} - \frac{2^{1/3}(-\phi_2^2 + 3\phi_1\phi_3)}{3\phi_3\left[-2\phi_2^3 + 9\phi_1\phi_2\phi_3 - 27\phi_0\phi_3^2 + \Delta\right]^{1/3}}\\
&+ \frac{\left[-2\phi_2^3 + 9\phi_1\phi_2\phi_3 - 27\phi_0\phi_3^2 + \Delta\right]^{1/3}}{3\,2^{1/3}\phi_3}
\end{aligned} \tag{26}$$

$$\begin{aligned}
Z_{22} = &-\frac{\phi_2}{3\phi_3} + \frac{(1 + i\sqrt{3})(-\phi_2^2 + 3\phi_1\phi_3)}{3\,2^{2/3}\phi_3[-2\phi_2^3 + 9\phi_1\phi_2\phi_3 - 27\phi_0\phi_3^2 + \Delta]^{1/3}}\\
&- \frac{(1 - i\sqrt{3})[-2\phi_2^3 + 9\phi_1\phi_2\phi_3 - 27\phi_0\phi_3^2 + \Delta]^{1/3}}{6\,2^{1/3}\phi_3}
\end{aligned} \tag{27}$$

Table 2 Regions and selected attractors for the membrane excitations study.

A	Region	Attractor	Lyapunov exponents
0.07	Frequency locking	Periodic	$\lambda_1 = 0.0000$, $\lambda_2 = -0.0121$, $\lambda_3 = -0.3461$, $\lambda_4 = -0.9725$, $\lambda_5 = -3.5927$
0.176	Quasi-periodicity	Quasi-periodic	$\lambda_1 = 0.0000$, $\lambda_2 = 0.0000$, $\lambda_3 = -0.4330$, $\lambda_4 = -1.7766$, $\lambda_5 = -2.7003$
0.614	Chaotic	Strange chaotic	$\lambda_1 = 1.2696$, $\lambda_2 = 0.0000$, $\lambda_3 = -0.2441$, $\lambda_4 = -2.0006$, $\lambda_5 = -3.9946$

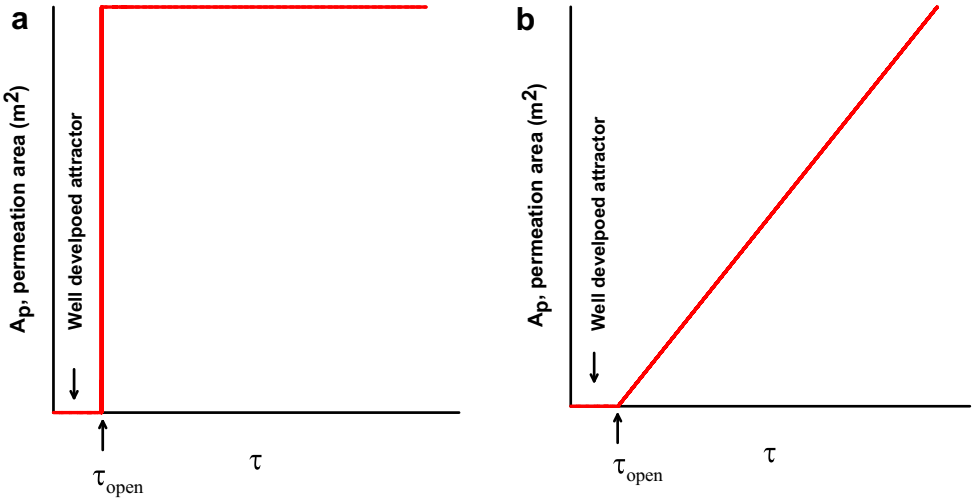

Figure 4 Schematic representation of: (a) the shock type membrane; (b) the linear dynamic membrane.

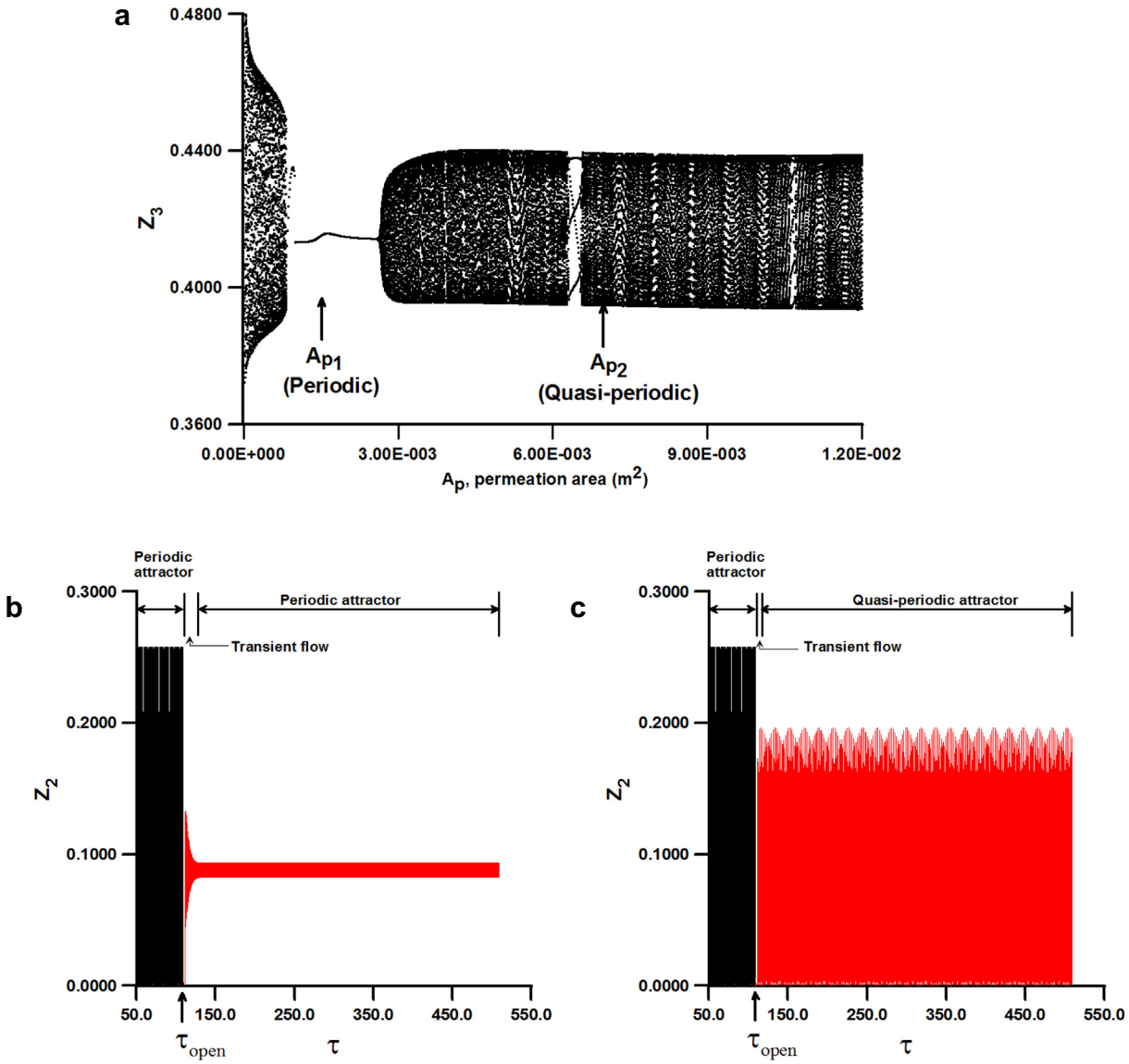

Figure 5 Influence of the shock type membrane on the periodic attractor in the frequency locking region: (a) A one-parameter stroboscopic Poincaré bifurcation diagram; (b) Time trace at $A_{p1} = 1.5 \times 10^{-3}$ m^2; (c) Time trace at $A_{p2} = 7.0 \times 10^{-3}$ m^2.

Please cite this article in press as: Abashar, M.E.E. The influence of membrane excitations on bioethanol production in a forced fermentor. Journal of King Saud University – Engineering Sciences (2016), http://dx.doi.org/10.1016/j.jksues.2016.10.004

$$Z_{23} = -\frac{\phi_2}{3\phi_3} + \frac{(1 - i\sqrt{3})(-\phi_2^2 + 3\phi_1\phi_3)}{3\,2^{2/3}\phi_3\left[-2\phi_2^3 + 9\phi_1\phi_2\phi_3 - 27\phi_0\phi_3^2 + \Delta\right]^{1/3}} - \frac{(1 + i\sqrt{3})\left[-2\phi_2^3 + 9\phi_1\phi_2\phi_3 - 27\phi_0\phi_3^2 + \Delta\right]^{1/3}}{6\,2^{1/3}\phi_3} \quad (28)$$

where:

$$\Delta = \sqrt{4(-\phi_2^2 + 3\phi_1\phi_3)^3 + (-2\phi_2^3 + 9\phi_1\phi_2\phi_3 - 27\phi_0\phi_3^2)^2} \quad (29)$$

The roots can be three distinct real roots, one distinct real root and two identical real roots, three identical real roots, and one real root and two complex conjugates. In this study, three distinct real roots are found. The values of the three steady states (Z_1, Z_2, Z_3, Z_4) as follows: SS_1 = (0.0056, 0.1620, 0.4138, 0.00011), SS_2 = (0.007, −0.0012, 0.4897, −0.00029) and SS_3 = (0.007, −0.0218, 0.4998, 0.00014). The second steady state (SS_2) and the third one (SS_3) show negative values, therefore physically excluded. The eigenvalues of the first steady state (SS_1) indicate that this steady state is unstable. This unstable steady state is surrounded by a stable periodic attractor as shown in Fig. 2. A shooting algorithm was employed to determine the natural period of this limit cycle. The autonomous reactor ordinary differential equations can be cast into matrix notations as follows:

$$\frac{d\boldsymbol{C}}{dt} = \mathbf{g}(\boldsymbol{C}, \psi), \quad \boldsymbol{C} \in \mathbb{R}^n \quad (30)$$

where $\boldsymbol{C}$ is the concentration vector, $\mathbf{g}$ is the vector of nonlinear functions and $\boldsymbol{\psi}$ is the parameters vector. A periodic solution must satisfy the following two boundary conditions**:**

$$\boldsymbol{C}(t = 0) = \boldsymbol{C}(t = P_n) \quad (31)$$

where P_n is the natural period. This two-point boundary problem is transformed to the following equivalent system of equations:

$$\mathbf{F}(\boldsymbol{C}, P_n) - \boldsymbol{C} = 0 \quad (32)$$

where P_n is unknown and $\mathbf{F}(\boldsymbol{C}, P_n)$ is obtained by integrating Eq. (30). Since infinite number of points on the limit cycle satisfies Eq. (31), an anchor equation is introduced to eliminate free translation in time (infinity of solutions):

$$G(\boldsymbol{X}, P_n) = 0 \quad (33)$$

Newton method is employed to solve Eqs. (32) and (33), where the Jacobian is given by:

$$\mathbf{J} = \begin{pmatrix} \frac{\partial \mathbf{F}}{\partial \boldsymbol{C}} - \mathbf{I} & \frac{\partial \mathbf{F}}{\partial P_n} \\ \frac{\partial G}{\partial \boldsymbol{C}} & \frac{\partial C}{\partial P_n} \end{pmatrix} \quad (34)$$

where $\mathbf{I}$ is the identity matrix and the derivatives $\partial\mathbf{F}/\partial\boldsymbol{C}$ are computed variationally. The importance of the natural period is that the forcing period will be a multiple of this period in the frequency locking region. Furthermore, the forcing period is usually employed to strobe the system to construct the Poincaré bifurcation diagram because it is always present in the response of the forced system.

5.2. Forced bioethanol fermentor without membrane

For the forced biosystem without membrane, the membrane permeation area is set to zero (A_p = 0). In this case we have two frequencies, namely the natural frequency ($\acute{\omega} = 2\pi/P_n$) and the forcing frequency ($\omega = 2\pi/P$). The ratio of the forcing frequency to the natural frequency is taken as a rational number of 2 ($\omega/\acute{\omega} = 2$). This point is the tip of a resonance horn. By increasing the normalized amplitudes three distinct regions are identified. The regions are frequency locking, quasi-periodic and chaotic. In order to choose the appropriate forcing amplitude for the chaotic region, a one-parameter stroboscopic Poincaré bifurcation diagram is developed for the forced system as shown in Fig. 3. We have used the normalized amplitude as a bifurcation parameter. As one can see that the chaos is developed by the famous Feigenbaum period doubling bifurcations. A normalized amplitude of 0.614 in the well developed chaotic region is selected as a center of excitations. Table 2 shows various selected attractors at specific normalized

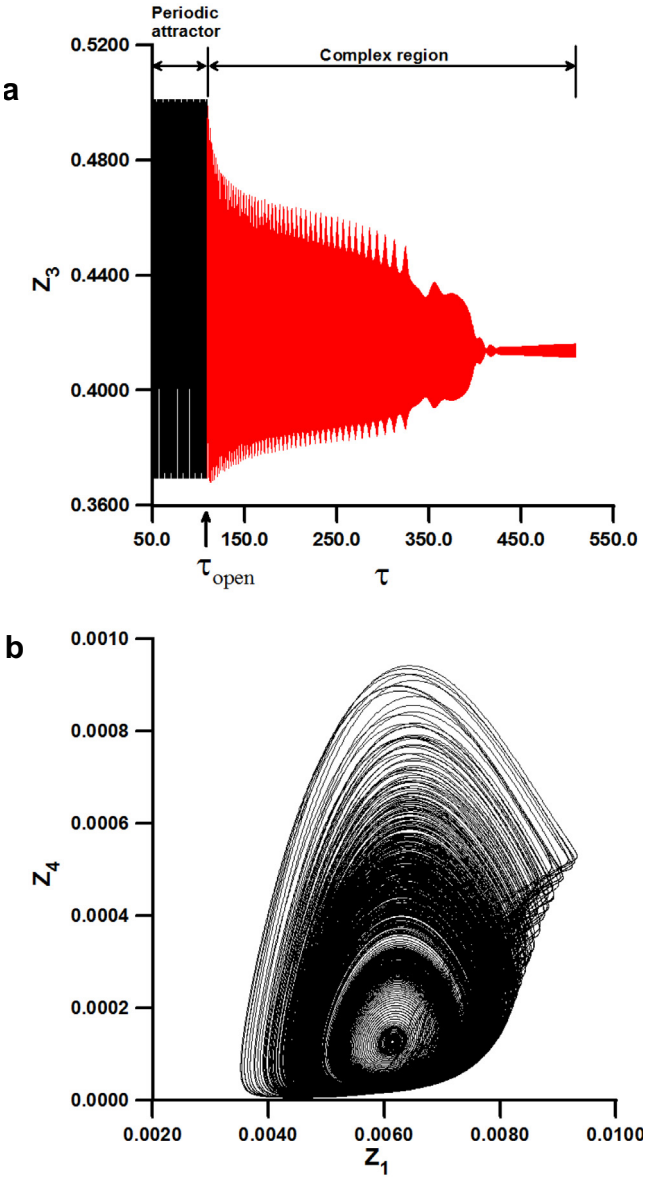

Figure 6 Influence of the linear dynamic membrane on the periodic attractor in the frequency locking region for the total membrane area of $A_p = 1.5 \times 10^{-3}$ m^2: (a) Time trace; (b) Phase plane of Z_4 vs. Z_1.

amplitudes in each region for the study. The influence of the membrane excitations on their dynamics is investigated in following sections.

5.3. Influence of the dynamic membrane on the forced bioethanol fermentor

The shock type and linear membrane configurations are implemented to excite the attractors shown in Table 2. Schematic representations of the shock type and linear dynamic membranes are presented in Fig. 4a and b, respectively. The shock type membrane represents instantaneous opening of the membrane i.e. very short time is taken to fully open the membrane as shown in Fig. 4a. The linear membrane presented in Fig. 4b represents linear opening of the membrane with time up to a fully open membrane i.e. the membrane attains the total area linearly.

5.3.1. Frequency locking region

In this region the forcing amplitude is small and the frequency locking occurs on a surface of a torus with periodicity twice the natural period of the limit cycle.

5.3.1.1. Effect of the shock type membrane. Here we will investigate the influence of the shock type membrane, i.e. the sudden opening of the membrane on the periodic attractor dynamics. A one-parameter stroboscopic Poincaré bifurcation diagram is shown in Fig. 5a. The membrane area (A_P) is considered as a bifurcation parameter. It is clearly shown that the membrane has a strong impact on changing the periodic dynamics. As illustrative examples the dynamic simulation is carried out at two selected permeation areas of $A_{p1} = 1.5 \times 10^{-3}\,m^2$ and $A_{p2} = 7.0 \times 10^{-3}\,m^2$. When the shock style membrane of an area of $A_p = 1.5 \times 10^{-3}\,m^2$ is applied the periodic attractor converges to a periodic attractor with periodicity the same as the forcing period and low amplitude oscillations as shown in the time trace presented in Fig. 5b. As the

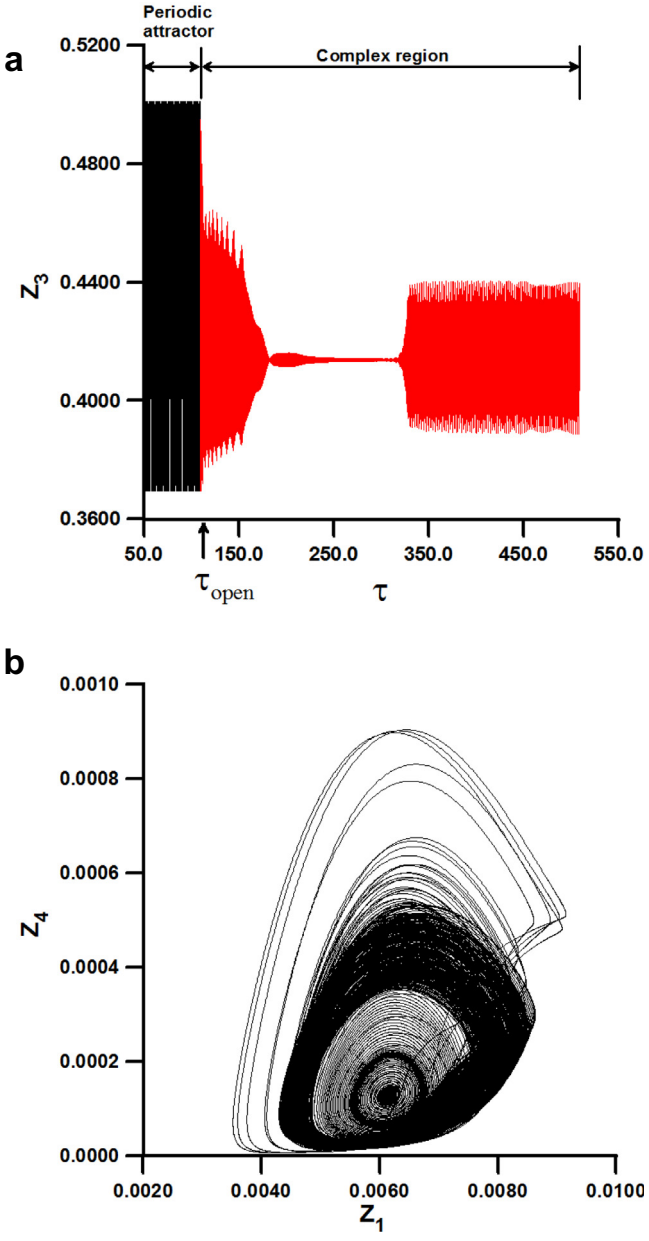

Figure 7 Influence of the linear dynamic membrane on the periodic attractor in the frequency locking region for the total membrane area of $A_p = 7.0 \times 10^{-3}\,m^2$: (a) Time trace; (b) Phase plane of Z_4 vs. Z_1.

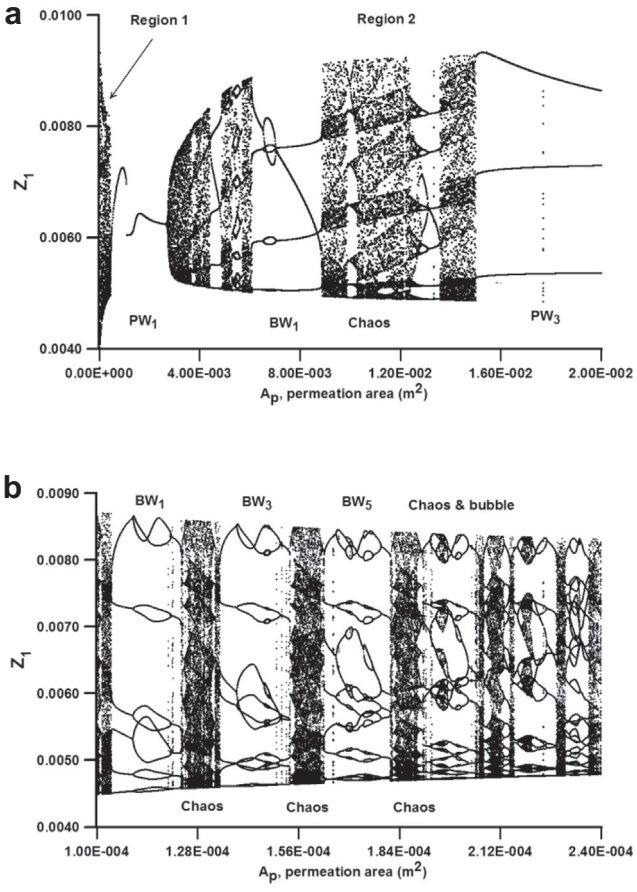

Figure 8 Influence of the shock type membrane on the quasi-periodic attractor in the quasi-periodic region: (a) A one-parameter stroboscopic Poincaré bifurcation diagram; (b) Enlargement of a part of the one-parameter stroboscopic Poincaré bifurcation diagram shown in Fig. 8a (complex region 1).

system is excited by a permeation area of $A_p = 7.0 \times 10^{-3}\,m^2$, the dynamics of the original periodic attractor is distorted to quasi-periodic oscillations as shown in the time trace in Fig. 5c. The corresponding spectrum of the Lyapunov exponents of this quasi-periodic attractor is ($\lambda_1 = 0.0000$, $\lambda_2 = 0.0000$, $\lambda_3 = -0.1380$, $\lambda_4 = -1.8811$, $\lambda_5 = -2.4005$).

5.3.1.2. Effect of the linear dynamic membrane. Now we considered the analysis of the biosystem when the periodic reactor is excited by the linear dynamic membrane. The influence of the membrane is investigated for two total permeation areas of $A_p = 1.5 \times 10^{-3}\,m^2$ and $A_p = 7.0 \times 10^{-3}\,m^2$. The larger the total membrane area implies the faster the membrane, i.e. the slope of the membrane openability function is increased.

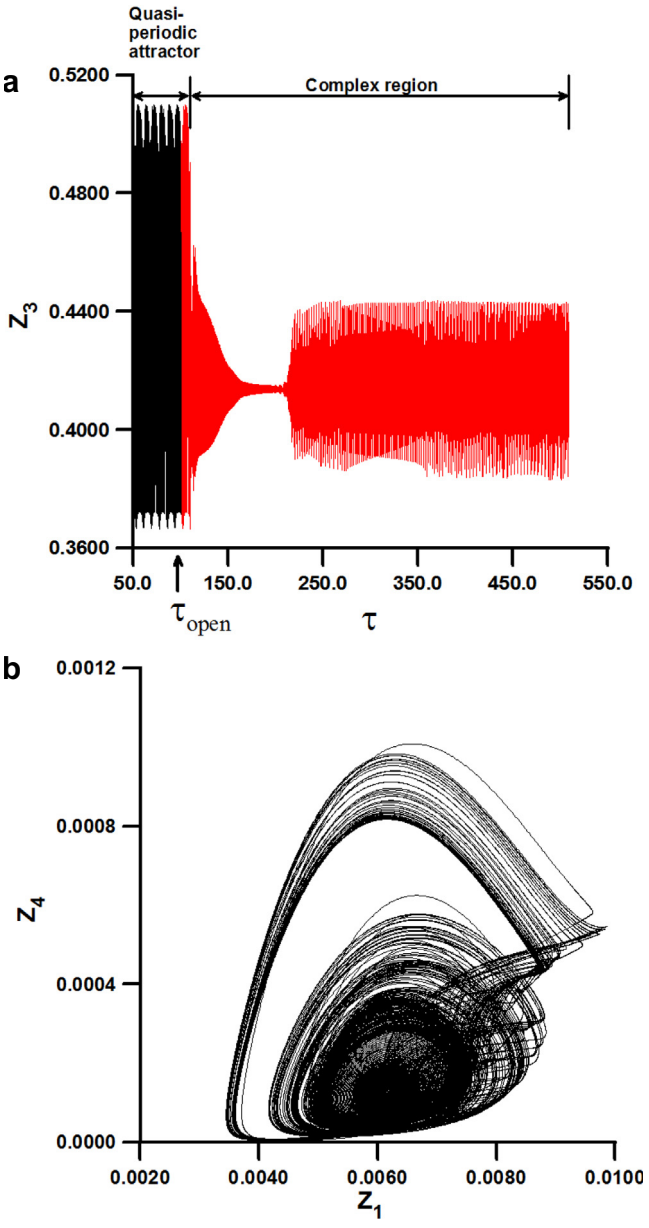

Figure 9 Influence of the linear dynamic membrane on the quasi-periodic attractor in the quasi-periodic region for the total membrane area of $A_p = 1.5 \times 10^{-3}\,m^2$: (a) Time trace; (b) Phase plane of Z_4 vs. Z_1.

When the membrane turns on linearly up to the final area of $A_p = 1.5 \times 10^{-3}\,m^2$, it is found that substantial complex dynamic changes occur as shown in the time trace and phase planes depicted in Fig. 6a and b, respectively. It is obvious that the attractor oscillates in a very complex manner. Fig. 7a displays the dynamics of the of forced system, when the linear dynamic membrane of an area equals to $A_p = 7.0 \times 10^{-3}\,m^2$ is employed to excite the periodic attractor. It should be observed that the system exhibits a complex dynamic behavior as shown in the time trace and phase planes presented in Fig. 7a and b, respectively.

5.3.2. Quasi-periodicity region

In this section the quasi-periodic attractor is excited by the adopted two membrane configurations.

5.3.2.1. Effect of the shock type membrane. The Poincaré bifurcation diagram for this case is shown in Fig. 8a. The diagram contains complex fascinated dynamical regions. Two apparent visible regions (region 1, region 2) separated by a large period 1 window (PW_1) are identified. An enlargement part of region 1 is shown in Fig. 8b. Fig. 8b demonstrates the evolution of the phenomenon of the bubble windows. It is interesting to note that the bubble windows show an incomplete odd sequence of 1, 3 and 5 (BW_1, BW_3, BW_5) according to the number of bubbles present. The truncated period doubling sequences

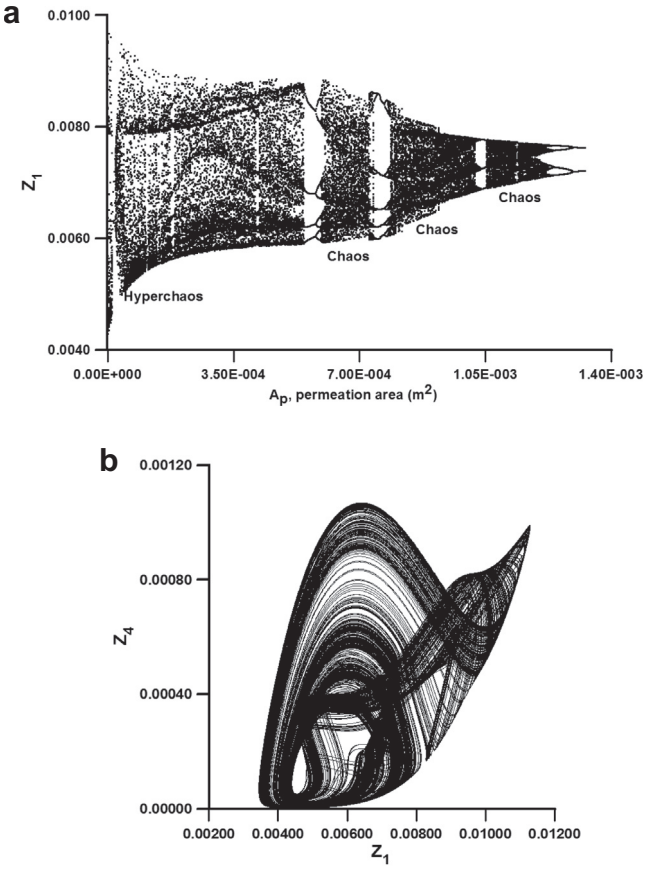

Figure 10 Influence of the shock type membrane on the chaotic attractor in the chaotic region: (a) A one-parameter stroboscopic Poincaré bifurcation diagram; (b) Phase plane of the hyperchaotic attractor at an area of $A_p = 2.0 \times 10^{-4}\,m^2$.

might be due to the complex interaction of the membrane permeation area with the forced system dynamics causing the system to change its bifurcation nature from period doubling sequences to period halving sequences. Also, chaotic bands exist. The chaos is developed by the famous Feigenbaum period doubling bifurcations and break down by period halving scenario. Another important observation is chaos followed by bubbles. Region 2 also contains complicated bifurcation structures such as a large bubble 1 window (BW_1) and chaotic attractors arise through period doubling scenario and suppressed by the period halving bifurcations.

5.3.2.2. Effect of the linear dynamic membrane. We implemented here the linear dynamic membrane of a total area of $A_p = 1.5 \times 10^{-3}\ m^2$. In this case, the quasi-periodic dynamics has been changed into a complex dynamic behavior as shown by the time trace and phase plane in Fig. 9a and b, respectively.

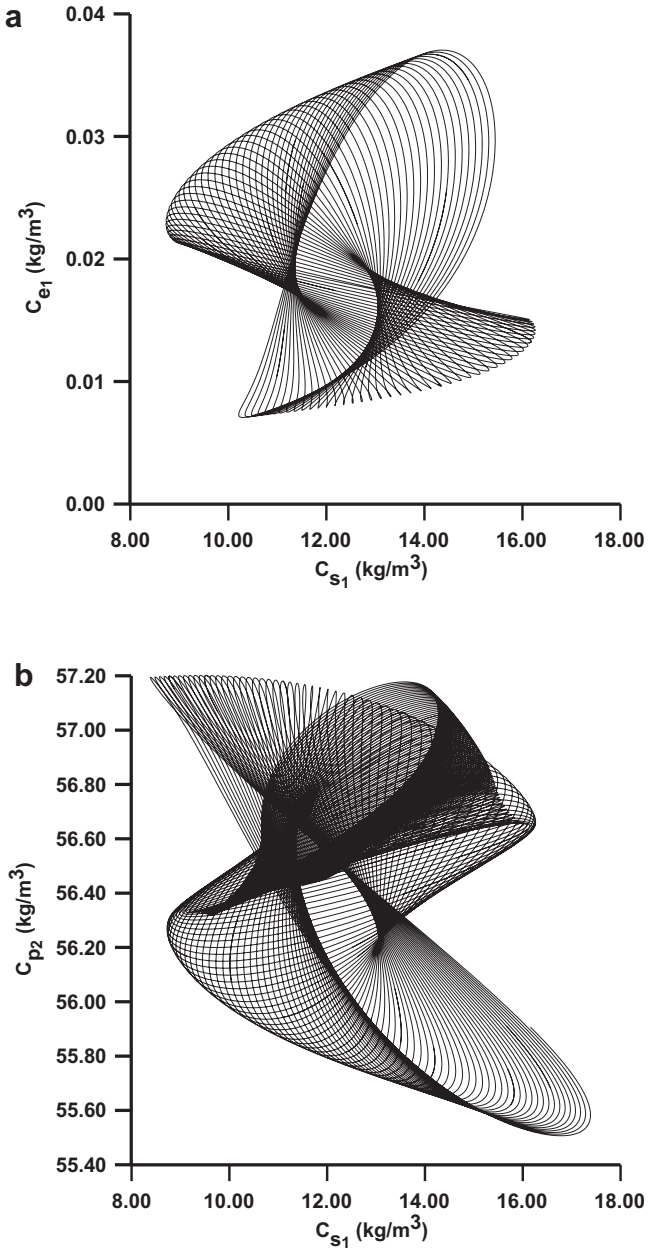

Figure 11 Examples of complex geometries in the hyperchaotic region shown in Fig. 10a: (a) C_{e1} vs. C_{s1}; (b) C_{p2} vs. C_{S1}.

5.3.3. Chaotic region

Chaos is a strange attractor that characterized by a single positive Lyapunov exponent as shown in Table 2.

5.3.3.1. Influence of the shock type membrane. Fig. 10 a shows the stroboscopic Poincaré bifurcation diagram due to the influence of the shock type membrane on the chaotic attractor. It is interesting to note that a hyperchaotic region evolves as well as chaotic regions. A phase plane of the hyperchaotic attractor at an area of $A_p = 2.0 \times 10^{-4}\ m^2$ is presented in Fig. 10b. The hyperchaos is characterized by at least two positive Lyapunov exponents. The Lyapunov spectrum of this hyperchaotic attractor is ($\lambda_1 = 1.0256$, $\lambda_2 = 0.8657$, $\lambda_3 = 0.0000$, $\lambda_4 = -1.1238$, $\lambda_5 = -2.3322$). It is interesting to note that complex geometrical structures are developed within the hyperchaotic region as displayed in Fig. 11a and b.

5.3.3.2. Influence of the linear dynamic membrane. When the linear dynamic membrane of a total area of $A_p = 1.5 \times 10^{-3}\ m^2$ is imposed on the chaotic dynamics, the response of the forced system is quite complex as shown in Fig. 12.

5.3.4. Potential benefits of membrane excitations

From an engineering point of view, we need to evaluate the merits and benefits of the implication of the membrane excitations on the dynamic performance of the forced fermentor. Table 3 shows the average ethanol yield compared to the autonomous (unforced) value for various bioreactor configurations. As one can see that for the forced system without membrane, the forcing can increase or decrease the ethanol yield depending on the final attractor. However, for the forced chaotic

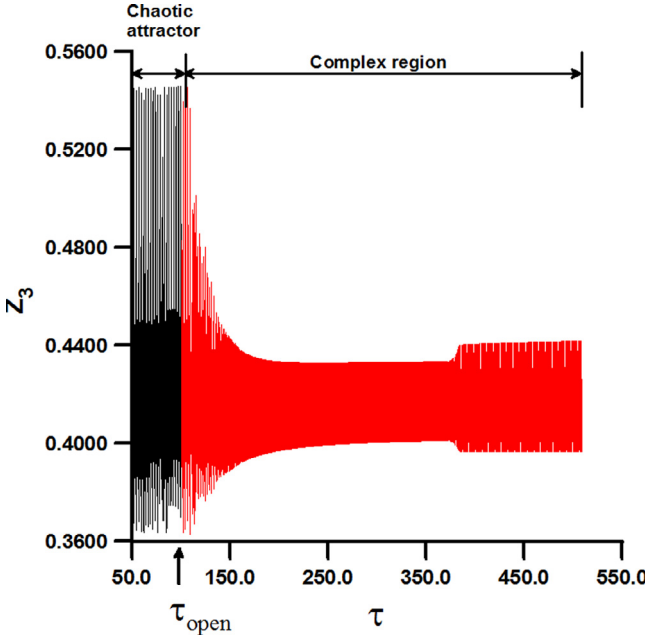

Figure 12 Time trace for the influence of the linear dynamic membrane on the chaotic attractor in the chaotic region for the total membrane area of $A_p = 1.5 \times 10^{-3}\ m^2$.

Please cite this article in press as: Abashar, M.E.E. The influence of membrane excitations on bioethanol production in a forced fermentor. Journal of King Saud University – Engineering Sciences (2016), http://dx.doi.org/10.1016/j.jksues.2016.10.004

Table 3 Percent average ethanol yield compared to the autonomous value for various biosystems configurations.

Forced bioreactor without membrane		Forced bioreactor with membrane			
		Membrane			
		Shock		Linear	
Attractor	Av. yield	Attractor	Av. yield	Dynamics	Av. yield
Periodic	−2.23%	Quasi-periodic	7.21%	Complex	9.26%
Quasi-periodic	1.65%	Chaotic	12.43%	Complex	14.22%
Chaotic	10.88%	Hyperchaotic	18.98%	Complex	19.29%

tic attractor significant improvement of ethanol yield of 10.88% is achieved. It is clearly shown that all membrane configurations achieve significant improvement in ethanol yield. It is interesting to note that when the shock type and linear membranes are imposed on the forced chaotic dynamics, the hyperchaos and the complex dynamics arise have increased the average ethanol yield to 18.98% and 19.29%, respectively. Furthermore, the membrane excitations can play a central role in the control systems to achieve the best desired reactor performance.

6. Conclusions

The present numerical results suggest that the membrane excitations and configurations have a profound effect on the dynamical behavior of the forced fermentor. The membrane excitation causes drastic dynamic changes of the original forced attractor accompanied by fascinated nonlinear phenomena. It appears that the complex regions of the chaos and hyperchaos could be of interest and have the potential for the best operation of the bioreactor. It seems that the linear dynamic membrane is superior to the shock type membrane. This investigation has demonstrated and highlighted the promising potential of the dynamic membranes implementation to enhance the biosystem performance. An area of a great potential needed to be explored is the influence of a vibrating dynamical membrane on the dynamics of unforced and forced biosystems.

Acknowledgements

This project was supported by King Saud University, Deanship of Scientific Research, College of Engineering Research Center.

References

Abashar, M.E.E., 2012. Dynamic phenomena in forced bioethanol reactors. Comput. Chem. Eng. 37, 172–183. http://dx.doi.org/10.1016/j.compchemeng.2011.11.013.

Abashar, M.E.E., 2011. Some complex dynamic features of a bioethanol fermentor excited by sinusoidal perturbations. Chem. Eng. J. 172, 386–398. http://dx.doi.org/10.1016/j.cej.2011.05.064.

Abashar, M.E.E., 1994. Bifurcation, Instability and Chaos in Fluidized Bed Catalytic Reactors (Ph.D. thesis). Salford University, UK.

Abashar, M.E.E., Elnashaie, S.S.E.H., 2011. Multistability, bistability and bubbles phenomena in a periodically forced ethanol fermentor. Chem. Eng. Sci. 66, 6146–6158. http://dx.doi.org/10.1016/j.ces.2011.08.040.

Abashar, M.E.E., Elnashaie, S.S.E.H., 2010. Dynamic and chaotic behavior of periodically forced fermentors for bioethanol production. Chem. Eng. Sci. 65, 4894–4905. http://dx.doi.org/10.1016/j.ces.2010.05.038.

Bruce, L.J., Axford, D.B., Ciszek, B., Daugulis, A.J., 1991. Extractive fermentation by Zymomonas mobilis and the control of oscillatory behavior. Biotechnol. Lett. 13, 291–296. http://dx.doi.org/10.1007/BF01041487.

Cristina, I., Astudillo, P., Ariel, C., Alzate, C., 2011. Importance of stability study of continuous systems for ethanol production. J. Biotechnol. 151, 43–55. http://dx.doi.org/10.1016/j.jbiotec.2010.10.073.

Garhyan, P., Elnashaie, S.S.E., 2004a. Utilization of mathematical models to investigate the bifurcation and chaotic behavior of ethanol fermentors. Math. Comput. Model. 39, 381–427. http://dx.doi.org/10.1016/S0895-7177(04)90514-6.

Garhyan, P., Elnashaie, S.S.E.H., 2004b. Bifurcation analysis of two continuous membrane fermentor configurations for producing ethanol. Chem. Eng. Sci. 59, 3235–3268. http://dx.doi.org/10.1016/j.ces.2004.05.003.

Ikegami, T., Yanagishita, H., Kitamoto, D., Haraya, K., Nakane, T., Matsuda, H., Koura, N., Sano, T., 1997. Production of highly concentrated ethanol in a coupled fermentation/pervaporation process using silicalite membranes. Biotechnol. Tech. 11, 921–924.

Jackson, E.A., 1989. Perspectives of Nonlinear Dynamics. Cambridge University Press, Great Britain.

Jobses, I.M.L., Egberts, G.T.C., Luyben, K.C.A.M., Roels, J.A., 1986. Fermentation kinetics of Zymomonas mobilis at high ethanol concentrations: oscillations in continuous cultures. Biotechnol. Bioeng. 28, 868–877.

Jobses, I.M.L., Egberts, G.T.C., Van Baalen, A., Roels, J.A., 1985. Mathematical modelling of growth and substrate conversion of Zymomonas mobilis at 30 and 35 °C. Biotechnol. Bioeng. 27, 984–995.

Kevrekidis, I.G., Aris, R., 1986. The stirred tank forced. Chem. Eng. Sci. 41, 1549–1560.

Kevrekidis, I.G., Schmidt, L.D., Aris, R., 1986. I. Some common features of periodically forced reacting systems. Chem. Eng. Sci. 41, 1263–1276. http://dx.doi.org/10.1016/S1874-5970(99)80019-8.

Kevrekidis, I.G., Schmidt, L.D., Aris, R., 2007. On the dynamics of periodically forced chemical reactors. Chem. Eng. Commun. 30, 323–330. http://dx.doi.org/10.1080/00986448408911136.

Mankin, J.C., Hudson, J.L., 1984. Oscillatory and chaotic behaviour of a forced exothermic chemical reaction. Chem. Eng. Sci. 39, 1807–1814. http://dx.doi.org/10.1016/0009-2509(84)80117-7.

Nishiwaki, A., Dunn, I.J., 1999. Analysis of the performance of a two-stage fermentor with cell recycle for continuous ethanol production using different kinetic models 4, 37–44.

Nomura, M., Bin, T., Nakao, S., 2002. Selective ethanol extraction from fermentation broth using a silicalite membrane. Sep. Purif. Technol. 27, 59–66. http://dx.doi.org/10.1016/S1383-5866(01)00195-2.

Parulekar, S.J., 2001. Forced periodic operations of continuous recombinant cell cultures subject to antibiotic selection pressure. Chem. Eng. Sci. 56, 6463–6484. http://dx.doi.org/10.1016/S0009-2509(01)00296-2.

Parulekar, S.J., 1998. Analysis of forced periodic operations of continuous bioprocesses—single input variations. Chem. Eng. Sci. 53, 2481–2502. http://dx.doi.org/10.1016/S0009-2509(98)00072-4.

Sinčić, D., Bailey, J.E., 1980. Analytical optimization and sensitivity analysis of forced periodic chemical processes. Chem. Eng. Sci. 35, 1153–1161. http://dx.doi.org/10.1016/0009-2509(80)85105-0.

Taylor, M.A., Kevrekidis, I.G., Kevrekidls, T.G., 1993. Couple, double, toil and trouble: a computer assisted study of two coupled CSTRs. Chem. Eng. Sci. 48, 2129–2149. http://dx.doi.org/10.1016/0009-2509(93)80088-8.

Villadsen, J., Nielsen, J., Lidén, G., 2011. Bioreaction Engineering Principles. Springer, US, Boston, MA. http://dx.doi.org/10.1007/978-1-4419-9688-6.

Please cite this article in press as: Abashar, M.E.E. The influence of membrane excitations on bioethanol production in a forced fermentor. Journal of King Saud University – Engineering Sciences (2016), http://dx.doi.org/10.1016/j.jksues.2016.10.004